PHILOSOPHICAL TRANSACTIONS A

rsta.royalsocietypublishing.org

Research

**Cite this article:** Tlidi M, Clerc MG, Escaff D, Couteron P, Messaoudi M, Khaffou M, Makhoute A. 2018 Observation and modelling of vegetation spirals and arcs in isotropic environmental conditions: dissipative structures in arid landscapes. *Phil. Trans. R. Soc. A* **376**: 20180026.
http://dx.doi.org/10.1098/rsta.2018.0026

Accepted: 9 June 2018

One contribution of 12 to a theme issue 'Dissipative structures in matter out of equilibrium: from chemistry, photonics and biology (part 2)'.

**Subject Areas:**
complexity

**Keywords:**
localized patches, dissipative structures, vegetation patterns

**Author for correspondence:**
M. Tlidi
e-mail: mtlidi@ulb.ac.be



# Observation and modelling of vegetation spirals and arcs in isotropic environmental conditions: dissipative structures in arid landscapes

M. Tlidi[1], M. G. Clerc[2], D. Escaff[3], P. Couteron[4], M. Messaoudi[5], M. Khaffou[5] and A. Makhoute[5]

[1]Département de Physique, Faculté des Sciences, Université Libre de Bruxelles (U.L.B.), CP. 231, Campus Plaine, Bruxelles, 1050 Belgium
[2]Departamento de Física, Facultad de Ciencias Físicas y Matemáticas, Universidad de Chile, Casilla 487-3, Santiago, Chile
[3]Complex Systems Group, Facultad de Ingeniería y Ciencias Aplicadas, Universidad de los Andes, Monseñor Alvaro del Portillo 12455, Las Condes, Santiago, Chile
[4]AMAP, IRD, CIRADm CNRS INRA, University Montpellier, Montpellier, France
[5]Faculté des Sciences, Université Moulay Ismail, Dynamique des Systemes Complexes et Simulation Numérique, B.P. 11201, Zitoune, Meknès, Morocco

DE, 0000-0001-9954-7687

We report for the first time on the formation of spirals like vegetation patterns in isotropic and uniform environmental conditions. The vegetation spirals are not waves and they do not rotate. They belong to the class of dissipative structures found out of equilibrium. Isolated or interacting spirals and arcs observed in South America (Bolivia) and North Africa (Morocco) are interpreted as a result of curvature instability that affects the circular shape of localized patches. The biomass exhibits a dynamical behaviour with arcs that transform into spirals. Interpretation of observations and of the predictions provided by the theory is illustrated by recent measurements of peculiar plant morphology (the alfa plant, or *Stipa tenacissima* L.) originated from northwestern Africa and the southern part of the Iberian Peninsula.

THE ROYAL SOCIETY PUBLISHING

This article is part of the theme issue 'Dissipative structures in matter out of equilibrium: from chemistry, photonics and biology (part 2)'.







## 1. Introduction

The physical mechanisms underlying non-equilibrium self-organization leading spontaneously to the formation of dissipative structures characterized by an intrinsic wavelength was proposed first by Ilya Prigogine in the context of reaction–diffusion systems [1–3]. This transition has been mathematically predicted in an earlier work by Turing [4]. The theoretical support of the Brussels school of non-equilibrium thermodynamics has rendered the work of Turing popular [5,6]. Dissipative structures have been observed in almost all fields of the natural sciences where the appearance of order and structure involves non-equilibrium exchanges of energy and/or matter (see overviews on this issue [7–19]). Biological systems and population dynamics, in particular, are domains of applicability of dissipative structures [20–22]. The vegetation patterns considered in this contribution belong to this class of non-equilibrium systems.

The formation of large-scale vegetation patterns in arid ecosystems is an area of interest for the study of dissipative structures. The first well-documented example of vegetation dissipative structures in arid ecosystems is bands often called tiger bush. They have been observed in aerial photographs that were taken in the early 1940s [23]. They are not detectable at the ground level because their pattern wavelength is of the order of 100 m. The patterned wavelength is defined as the sum of the widths of densely (or sparsely) populated patches and of their spacing. The theory of vegetation patterns has been established by Lefever & Lejeune [24]. In extreme conditions where resources become scarce, the vegetation tends to self-organize to optimize water or nutrient uptake. Indeed, individual plant strives to increase resources (water and/or nutrient) uptake by spreading their roots over a greater territory. As a consequence, the degree of overlap of plant root systems is increased through the competition between plants for resources. This process tends to inhibit the increase of the biomass (negative feedback). On the other hand, there are other factors such as accumulation of resources in the neighbourhood of the plants, the reciprocal sheltering of neighbouring plants, and the provision of shade that tends on the contrary to increase the water availability in the soil and thus to improve the biomass production (positive feedback), also known as facilitation. The facilitative process operates on a small spatial scale of the order of the aerial part of the individual plant while longer ranges have been reported for root competition. These two complementary processes that operate at different spatial scales allow for the stabilization of vegetation patterns. For the vegetation patterns to form even in isotropic and uniform environmental conditions, it is indeed necessary that competitive interactions be of longer range than facilitative interactions [24–26]. The effect of water transport by below-ground diffusion and/or above-ground run-off coupled to the dynamics of the biomass has been proposed [28–33]. Other approaches have been based on the constructive role of environmental randomness as a source of noise-induced transitions leading to the formation of dissipative vegetation patterns [34,35]. The morphologies of periodic vegetation patterns emerging from the symmetry-breaking instability follow the generic sequence gaps $\Longleftrightarrow$ stripes (labyrinth) $\Longleftrightarrow$ spots as the level of the aridity is increased [25,26]. This generic sequence has been recovered from other models that incorporate water transport in the modelling [31,36].

Dissipative structures are not always periodic. Spatial localization is a patterning phenomenon arising from the bistability between the bare state and the periodic patchy vegetation state. The structures can be localized and aperiodic in space consisting of stationary isolated, circular patches fixed on a bare soil. These circular patches can be either isolated or randomly distributed in a given territory [37,38]. They can consist of localized spots of bare soil often called localized gaps, randomly distributed in an otherwise uniform vegetation cover [39]. This self-organized patchiness can become unstable with respect to the curvature instability that affects the circular

shape, leading to the self-replication regime [40,41]. This is a well-documented issue in various fields of nonlinear science such as biology, hydrodynamics and nonlinear optics [17–19].

We report here on the formation of spirals and arcs like vegetation patterns in isotropic and uniform environmental conditions. Nonlinear science abounds with examples of spiral waves. The discovery of the Belousov–Zhabotinski reaction allows the generation of rotating spiral waves around their cores [42–44]. The curvature dependence of the wave propagation velocity of spiral waves allows for transitions from a stable flat wave to a folded one and then to spiral turbulence [45]. It is now generally admitted that excitability [42–44] is the main mechanism to explain the formation of rotating spiral waves. The vegetation spirals presented in this contribution are not waves and they do not rotate. In the context of ecology and plant ecology, spiral patterns are not yet documented for any type of vegetation. They have never been reported in nature nor predicted by mathematical modelling. We use the generic interaction-redistribution model based on the relationship between the structure of individual plants and the nonlocal interactions existing within the plant community. This single variable model for the plant biomass density allows us to test a set of predictions for resources-limited ecosystems. We show that for moderate aridity conditions, a single or more localized patch can exhibit a curvature instability. During time evolution, the biomass in the central portion of the localized patch decays followed by the transition to the formation of a doughnut-like shape. This structure breaks down into arcs of vegetation and transforms into spiral-like patterns. Spiral-like and arc patterns are observed in many arid and semi-arid regions of South America (Bolivia) and northwestern Africa (Morocco) as shown in figure 1 and figure 2. We present field measurements of a particular plant morphology (the alfa grass, or *Stipa tenacissima* L.). Field measurements allow us to provide the realistic estimation of biomass density of the above- and the below-ground parts, and of all the model parameters including the full lateral roots extension and the facilitative range of interactions.

The paper is organized as follows. After an introduction, we present in §2 field observations and the characterization of the vegetation patterns in terms of their facilitative and competitive interactions. A precise measurement of the biomass is also provided. The results are presented in §3. The generic interaction-redistribution and the numerical simulation leading to the formation of spirals and arcs are discussed in §4. We conclude in §5.

## 2. Field measurements and parameter assessment

We consider the alfa vegetation (or *Stipa tenacissima* L.) in the high steppe plateau in eastern Morocco. This plant appears as grass tussocks and is reported as dominant over extensive areas in northern Africa (Algeria, Libya, Tunisia, Morocco) and southwest Europe (Spain, Italy). Notably, the species impressively dominates some parts of the uplands in Algeria and Morocco. The corresponding area over all of northern Africa is large and was estimated in the 50 s as about 8 millions hectares although remaining surfaces seem now restricted to just more than 3 million hectares [46]. Alfa is used to produce objects such as baskets, carpets and ropes (traditional craft applications) and can also be manufactured into high-quality paper (cigarettes, bank notes) or into thermal and phonic insulation boards. Above all, alfa-dominated steppes are quintessential grazing lands for livestock (mainly sheep but also goats and camels) all over northern Africa. Such pasture lands meet most of the food needs of tens of millions of herds of small ruminants [46]. Degradation induced by over-stocking and perhaps droughts is reported to be alarming in many regions [46–48]. In comparison, most European alfa grasslands no longer experience important grazing [49,50]. Alfa is a tall perennial grass forming tussocks that reach heights of 0.5 m to more than 1 m in the centre of the tuft [46,51]. Alfa grasslands experiencing low to moderate grazing levels are reported to display above-ground phytomass (AGP) in the range 5000–10 000 kg of dry matter per ha (DM/ha), among which the *Stipa tenacissima* species often accounts for more than 90% [46]. This corresponds to densities in the range of 7000–9000 tufts per ha (exceptionally 10 000, [47,52]). In Spain, total carbon storage in a well-preserved alfa sward and underlying soil was found to exceed 40 000 Kg C $ha^{-1}$ [50]. In the alfa tufts, leaves exhibiting living green

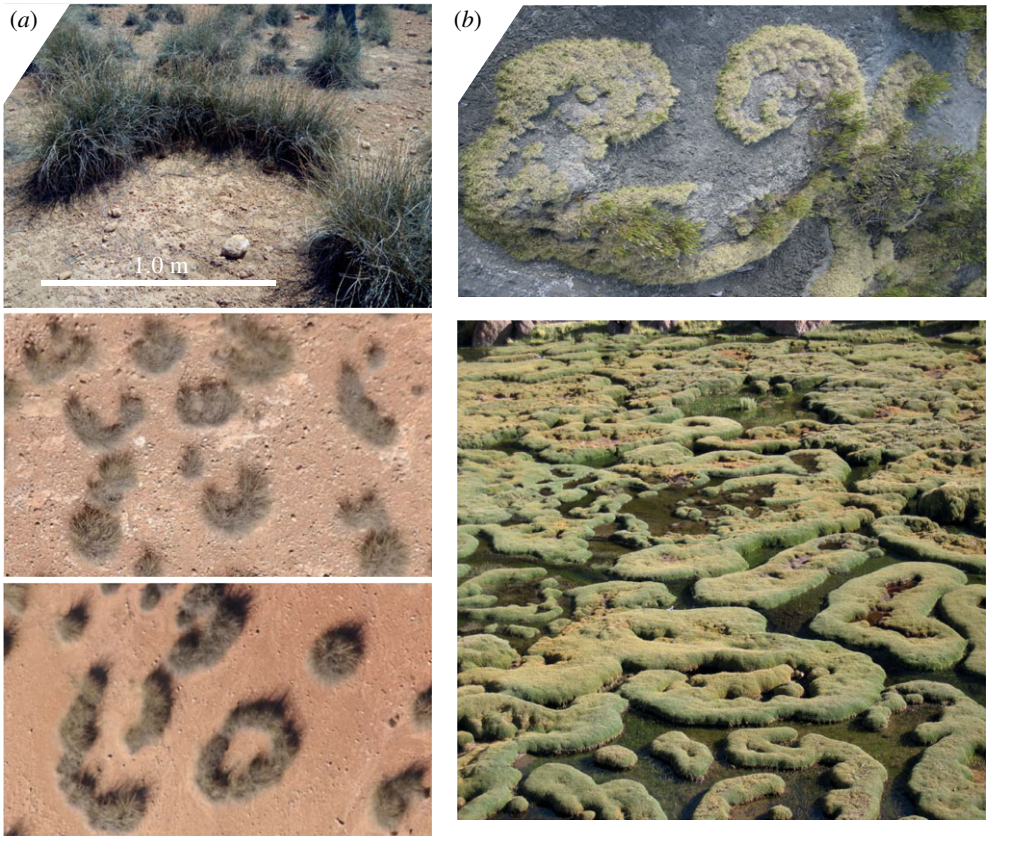


**Figure 1.** Observations of spirals and arc-like vegetation patterns in (*a*) Morocco, Enjil region (Boulmane Province), and in (*b*) Bolivia, courtesy of Eric Louvergneaux, Lille University, France who provides the first observation of spiral vegetation structures in 2008. (Online version in colour.)

tissue generally do not represent more than 20% of total AGP and there is a dominant share of dead leaves remaining attached to the tuft basis (i.e. necromass or '*fatras*' in French). Appropriate grazing regimes may reduce the necromass portion but generally not under 60%. Saturation by necromass is sometimes presented as the cause of dieback in the tuft centre that progressively makes tussocks become ring-shaped and eventually fragment [52]. This phenomenon, named *circination* in French, is a well-known feature of the species [46,52]. The causes and consequences of central dieback and tuft fragmentation are still controversial in the literature and we will address this important issue in the present paper by modelling tuft dynamics.

## (a) Study area

We carry out measurements in the steppe highlands of the province of Boulmane of north-central Morocco. All measurements have been performed in the commune of Enjil located in the steppe plains. It is considered as a crossroads between the east and northeast on the one hand, and the southwest of Morocco on the other hand. The field site is located at an altitude of 2029 m. The average annual temperature is 20.5°C, with an average of daily minima of 30.0°C and an average of daily maxima of 38°C. The region of Fès-Boulmane experiences two types of climate: in the north, the climate is Mediterranean, influenced by the mountains, especially their southern slopes, and rainfall reaches 40 cm per year. In the south, the climate is continental and subject to Saharan influences and rainfall is 10 cm per year, which is in the lower part of the rainfall range reported for the occurrence of alfa grasslands [46–48].

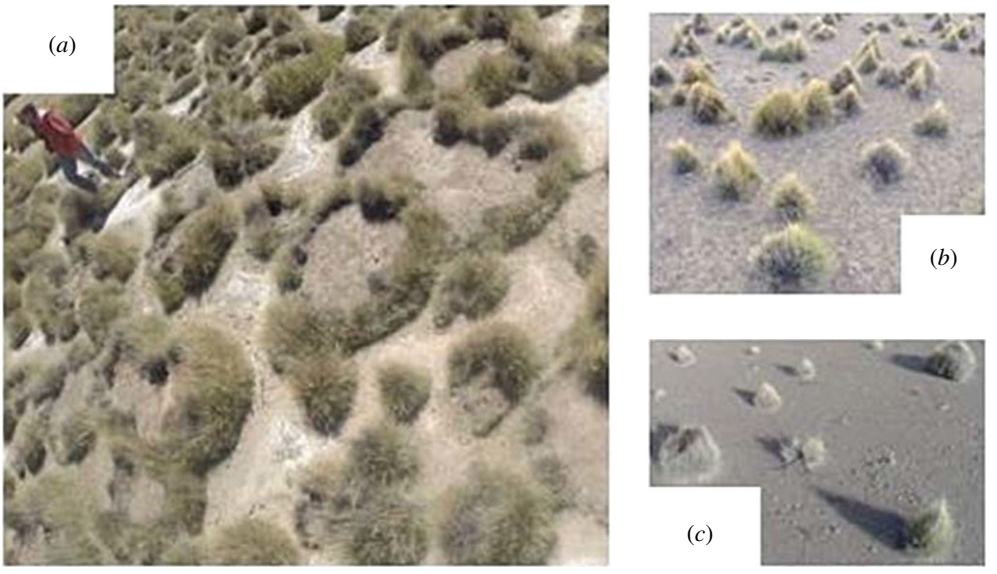


**Figure 2.** Spatial patterns observable for *Festuca orthophylla* L., a widespread tussock-forming grass species in the high elevation zones of the Andes. System of high cover dominated by ring-shaped and spiral-like structures. (*b*) System of intermediate cover made of compact tufts. (*c*) Low cover system with compact tufts of varying sizes. Photos from Fabien Anthelme (IRD) in the Sajama National Park, in Bolivia (see [53] for context). (Online version in colour.)

## (b) Methods

Measurements have been performed in the field and in the laboratory. Three plots of $100\,m^2$ ($10\,m \times 10\,m$), $400\,m^2$ ($20\,m \times 20\,m$) and $900\,m^2$ ($30\,m \times 30\,m$) surfaces were delineated on a flat topography inside the alfa steppe of Enjil. In the plots, we have randomly selected 33 alfa tussocks. This campaign of field measurements was carried out during May 2017. It consisted in measuring tuft maximal height and above-ground radius, as well as cautiously excavating root systems to measure their lateral extensions. Then we transported the sampled alfa plants to the laboratory located at the Moulay Ismael university (Meknés, Morocco). In the laboratory, we oven-dried plant material at 70°C before weighting to obtain dry matter weights. Each sampled plant was divided into three parts: roots, above-ground living leaves and dead leaves remaining attached to the plant (i.e. necromass or fatras), as is shown in figure 4.

# 3. Results

The average dry weight of the sampled tufts was 378.1 and 494.3 gr of dry matter (DM) for above-ground live and dead phytomass, respectively (see distributions in figure 3*a*,*b*). Average below-ground phytomass was 250.1 gr DM per tuft. The ratio of live to dead above-ground phytomass was 0.77 among a total above-ground phytomass of 873.1 gr DM per tuft. By counting, we assessed the alfa plant density as 0.44 tufts per $m^2$ and thereby reached an estimate of $3.84\,t\,ha^{-1}$ for the total above-ground phytomass. The average total phytomass (including roots) was 1123.2 gr DM per tuft, yielding $4,94\,t\,ha^{-1}$. The distributions of above-ground and rhizospheres radii for the 33 tussocks excavated and harvested are presented in figure 3*c*,*d*. The alfa plants at Enjil were characterized by an average aerial radius (above-ground part of the plant) of 54.1 cm and an average root radius (below-ground part of the plant) of 136.8 cm. These two values directly relate to the model parameters $L_a$ and $L_2$ (see point 4), respectively, and are key parameters in the way in which we model the spatial dynamics of alfa vegetation.

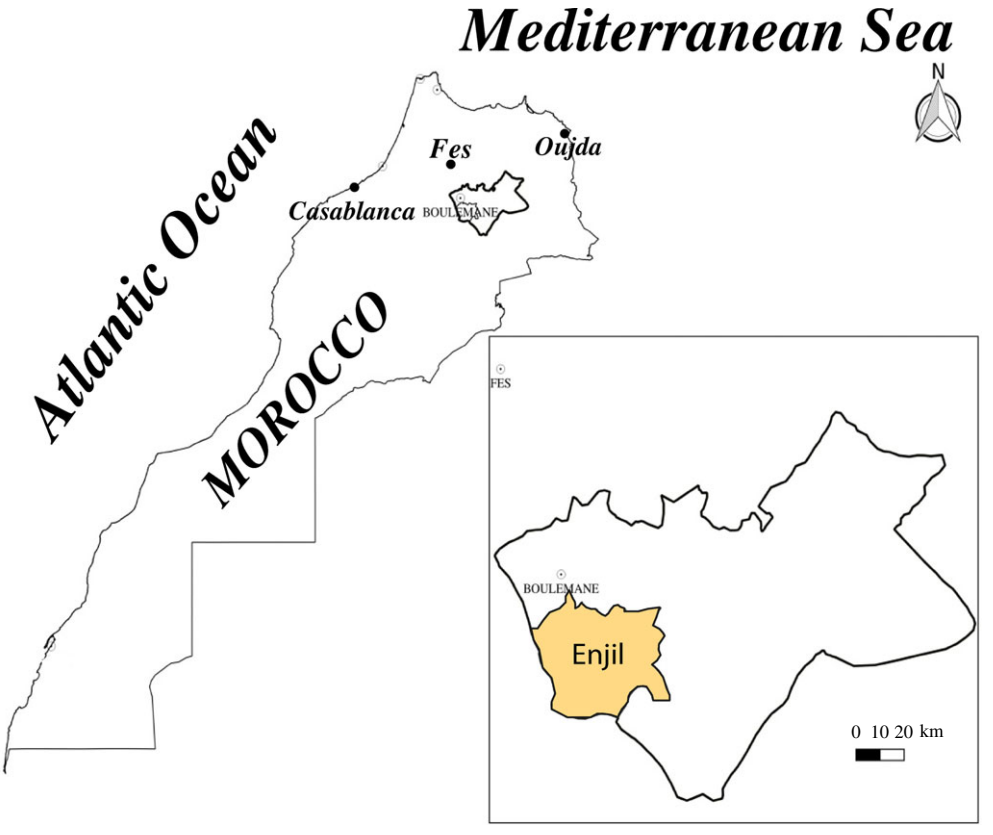


**Figure 3.** The geographical location of the study area. (Online version in colour.)

## 4. Interaction-redistribution model

We consider the generic interaction-redistribution model based on the relationship between the structure of individual plants and the nonlocal interactions existing within the plant community. In this approach, the vegetation pattern formation process originates from interactions intrinsic to the vegetation dynamics (facilitation and competition), rather than from extrinsic, environmental causes. This approach has been validated by field measurements for two type of plants: *Festuca orthophylla* L. [53] and *Combretum micranthum* G. Don [54–56]. *Festuca orthophylla* is a tall dryland tussock of the Andean Altiplano that shares many characteristics with alfa.

Let $b(\boldsymbol{x}, t) \in [0, 1]$ be the biomass density that evolves at time $t$ for an element of surface centred on a point $\boldsymbol{x}$ in two-dimensional Euclidean plane. This is the state variable of the system that describes the biomass of vegetation (here mainly the alfa, focal species) for a given species. Environmental conditions are uniform and isotropic. The time scale associated with the evolution of individual plants is much faster compared to the time scale over which evolves the whole community. The landscape described above is dominated by the alfa plant. The vegetation is described in terms of the total biomass. The biomass is composed of two parts: the above- and the below-ground biomass which are merged into a single variable $b(\boldsymbol{x}, t)$ (total biomass density for simplicity). The generic interaction-redistribution model reads [57]

$$\partial_t b = \exp(F_1)(b + dF_D)(1 - F_2) - \mu b. \tag{4.1}$$

The first term, $F_1$, only describes the biomass increase through plant growth that benefits from the accumulation of resources and decrease of evaporation near other plants. The second term, $F_D$, only describes the source of biomass arising from the propagation of vegetation by seed

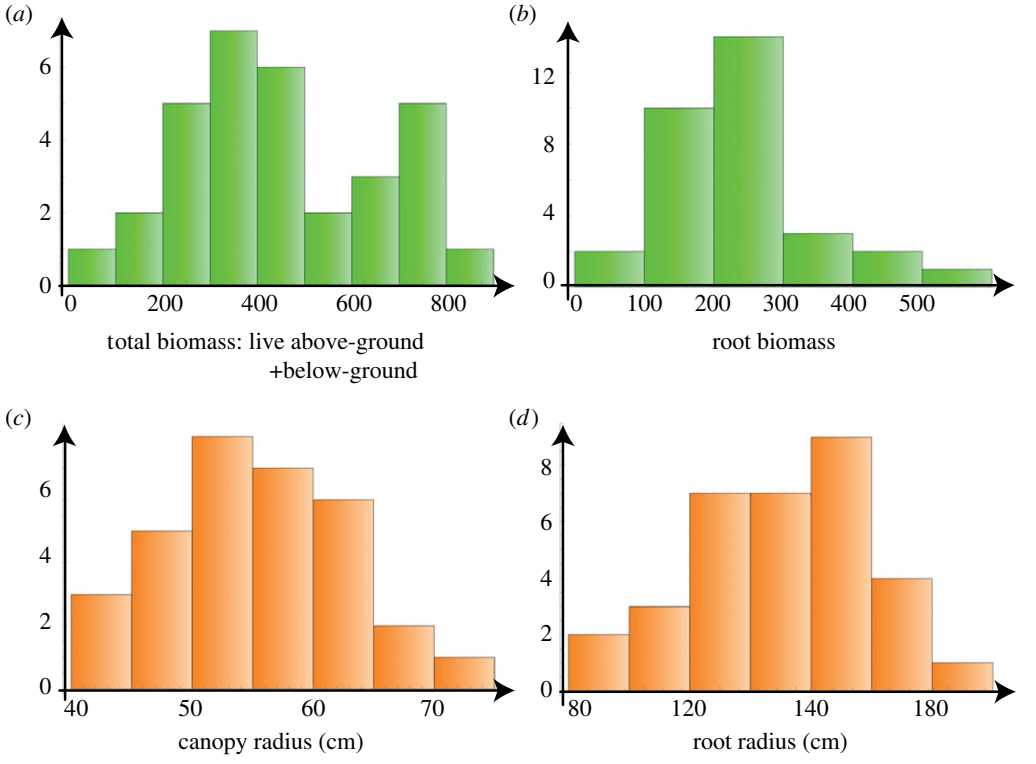


**Figure 4.** (*a*) Frequency distribution of values for above-ground live biomass per sampled tuft; (*b*) Frequency distribution of values for below-ground live biomass by sampled tuft. Abscissa in both (*a*) and (*b*) in gr of dry matter. (Online version in colour.)

production and dispersion. The competition for resources (water and/or nutrient) which hinders the development of the biomass via the logistics factor $F_2$. The explicit forms of $F_1$, $F_2$ and $F_D$, are

$$F_1 = \frac{1}{2\pi L_a^2} \int \exp\left(-\frac{|x'|}{L_1}\right) b(x+x',t)\, \mathrm{d}^2x',$$

$$F_2 = \frac{1}{2\pi L_2^2} \int \exp\left(-\frac{|x'|}{L_2}\right) b(x+x',t)\, \mathrm{d}^2x'$$

and

$$F_D = \frac{1}{\pi L_D^2} \int \exp\left(-\frac{x'^2}{L_D^2}\right) b(x'+r,t)\, \mathrm{d}^2x',$$

For a more detailed description of the model see Lefever & Turner [57]. The mortality-to-growth rate ratio $\mu$ increases with the aridity: a drier environment usually implies a lower growth rate and, possibly, higher mortality of the biomass. The parameter $d$ measures the strength of seed dispersion. The lengths $L_a$, $L_1$, $L_2$, $L_D$ of the non-local interactions represent the effective radius of the surface that occupies a mature plant, the facilitative range, the competitive range, and the seed dispersion range, respectively. The range of all non-local interactions between plants depends on the stage of development of the vegetation. It is obvious that mature plants affect a greater territory than young seedlings. The ranges of the competitive and facilitative interactions depend on the total plant biomass. In what follows we assume that all plants are mature and we, therefore, neglect the allometric factor that links interaction ranges to biomass (as in Lefever *et al.* [56]) so as to indirectly express age classes. It means that, for simplicity, we consider that all interaction lengths are constants.

The homogeneous steady states of equation (4.1) are solutions of

$$\exp(\Gamma^2 b_0)(1+d)(1-b_0)b_0 - \mu b_0 = 0, \tag{4.2}$$

where $\Gamma = L_1/L_a$. The trivial solution of equation (4.2) is $b_0 = 0$. When decreasing the aridity parameter $\mu$, the state $b_0 = 0$ that represents a territory totally devoid of vegetation becomes unstable for $\mu < 1 + d$. This bare state becomes stable when $\mu > 1 + d$. Non-trivial solutions of equation (4.2), that represent uniformly vegetated states, obey the equation

$$e^{\Gamma^2 b_0}(1 - b_0) = \frac{\mu}{1+d}. \tag{4.3}$$

Two cases must be distinguished according to the value of the parameter $\Gamma$. If $\Gamma > 1$, the branch of the uniformly vegetated state extends up to the turning point or a tipping point. In this case, there exist a range of the aridity parameter where we have a bistable behaviour between bare state and uniformly vegetated cover. If $\Gamma < 1$, there is only one uniformly vegetated state that decreases in a monotonous way as a function of aridity and coincides with the bare state at $\mu = 1 + d$.

The analysis of the stability of the uniformly vegetated state with respect to perturbations of the form $\exp[i\boldsymbol{k}\cdot\boldsymbol{x} + \lambda(k)t]$ around the homogeneous vegetated cover $b_0$ leads to the characteristic equation

$$\lambda(k) = \mu\left\{\frac{\Gamma^2 b_0}{(1+(kL_1)^2)^{3/2}} + \frac{1+d\exp(-(kL_D/2)^2)}{1+d} - \frac{b_0}{(1-b_0)(1+(kL_2)^2)^{3/2}} - 1\right\}. \tag{4.4}$$

We are interested in the situation where the homogeneous vegetated cover exhibits a symmetry breaking instability leading to the formation of periodic structures. The eigenvalue $\lambda$ vanishes for a finite wavenumber $k = k_c$. Above the threshold associated with this instability, there exists a finite band of Fourier modes $k_-^2 < k^2 < k_+^2$. In order to illustrate this result, we fix the parameters $L_a = 1.25$, $L_1 = 2$, $L_2 = 2.8125$, $L_D = 2.5$, and $d = 0.5$, and let the aridity parameter $\mu$ be the control parameter. Figure 5 displays our results. In the left panel is shown the spatially uniform state as a function of the control parameter $\mu$: continuous blue curves represent stable states; dashed blue curves represent states that are unstable even for spatially homogeneous perturbations ($k = 0$); while dashed red curves represent states that are unstable only for finite wavelength perturbations. In the right panel is displayed the spectrum equation (4.4) for the upper branch: Below the critical point; at the critical point $\mu_{c1} \cong 2.57722$ when the first mode $k_c \approx 0.477$ becomes unstable; above the critical point but below the saddle point; and just at the saddle point $\mu_{c2} \approx 2.78837$, where even $k = 0$ is unstable because the upper branch collides with the lower one. In order to figure out which are the unstable modes depending on the biomass, we have solved the equation $\lambda(k) = 0$, which gives us the functions

$$b_\pm(k) = \frac{-B(k) \pm \sqrt{B(k)^2 - 4A(k)C(k)}}{2A(k)}, \tag{4.5}$$

where

$$A(k) = \frac{\Gamma^2}{\left(1+(kL_1)^2\right)^{3/2}},$$

$$B(k) = \frac{1+d\exp\left(-(kL_D/2)^2\right)}{1+d} + \frac{1}{\left(1+(kL_1)^2\right)^{3/2}} - \frac{\Gamma^2}{\left(1+(kL_1)^2\right)^{3/2}} - 1$$

and

$$C(k) = 1 - \frac{1+d\exp\left(-\left(\frac{kL_D}{2}\right)^2\right)}{1+d}.$$

Numerical simulations of equation (4.1) in two-dimensional systems are performed for the parameters $L_a = 1.25$, $L_1 = 2$, $L_2 = 2.8125$, $L_D = 2.5$, $d = 0.5$ and $\mu = 2.9$. We use periodic boundary conditions in both $x$ and $y$ directions. The initial condition consists of circular localized patches.

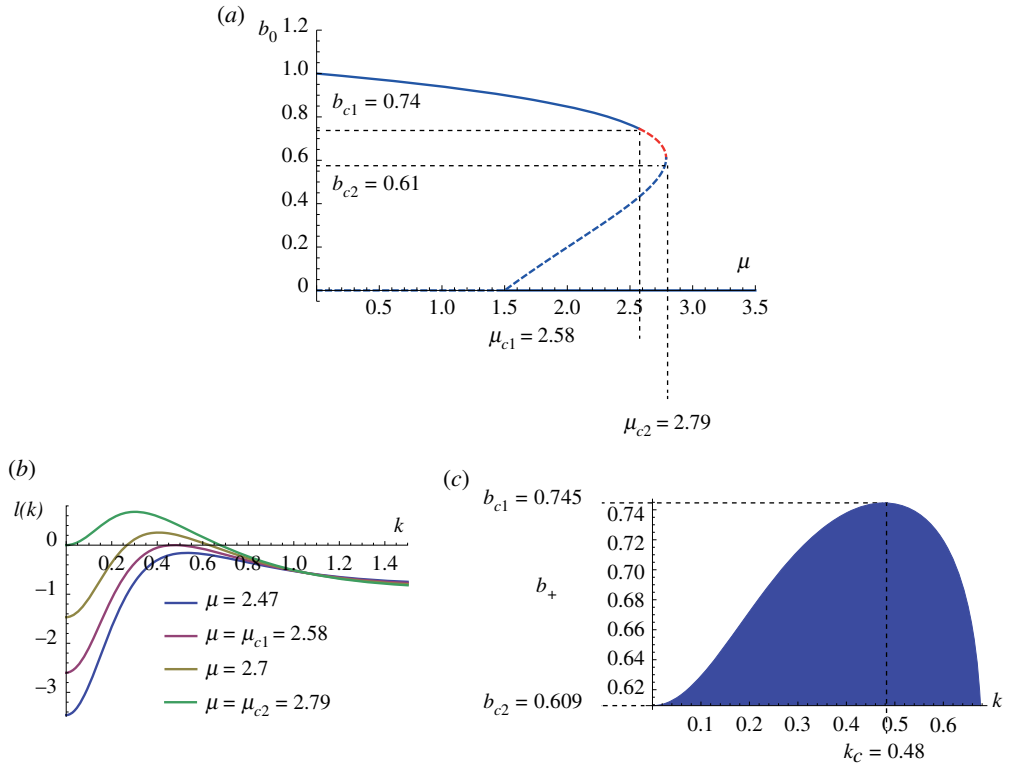


**Figure 5.** Linear stability of the uniformly vegetated states, for $L_a = 1.25$, $L_1 = 2$, $L_2 = 2.8125$, $L_D = 2.5$ and $d = 0.5$. (*a*) Homogeneous solutions as a function of the aridity parameter $\mu$: continuous blue curves represent stable states; dashed blue curves represent states that are unstable even for spatially homogeneous perturbations; while dashed red curves represent states that are unstable only for finite wavelength perturbations. (*b*) The spectrum equation (4.4) for the upper branch. Unstable waves numbers for biomass densities at the upper branch. The dark area corresponds to unstable Fourier modes, the upper perimeter of this area is the solution $b_+(k)$ of equation (4.5). (Online version in colour.)

These circular patches become unstable and display transitions towards the formation of a doughnut-like shape. The central part of these structures is made of almost bare soil. In the course of time, arc-like structures are formed as shown in figure 6. Arc-like vegetation structures have been reported in anisotropic environmental conditions owing to atmospheric factors such as wind and light or geomorphological factors such as ground surface or topography and slopes as in [24]. In this work, it has been shown that the width of vegetated bands increases when environmental conditions become more arid and that patterns formed of stripes oriented parallel to the direction of a slope are static. However, patterns which are perpendicular to this direction exhibit an upslope motion [24]. Earlier approaches based on cellular automata have been proposed for the analysis of vegetation patterns where the landscapes are modelled as the tessellation of rectangular cells [58–61]. Arcs of vegetation have been analysed essentially under anisotropic environmental conditions in Somalia [62], in Sudan [63], and in Burkina Faso [64]. In Spain, [49] reported alfa form 'rings' on a plateau and 'kidney' or 'elongated shapes' on slopes.

During time evolution, arcs transform into spiral-like patterns as shown in figure 6. The biomass increases in the course of time and contributes to the repopulation of the whole territory accessible to vegetation. The spirals and arcs reported here are not rotating structures and are transient. The longtime dynamics leads to the hexagonal structures formed by several patches, as shown in figure 6. If we choose an initial condition consisting of more numerous localized patches, the dynamics lead to the formation of arcs and spirals as shown in figure 7. It is worth

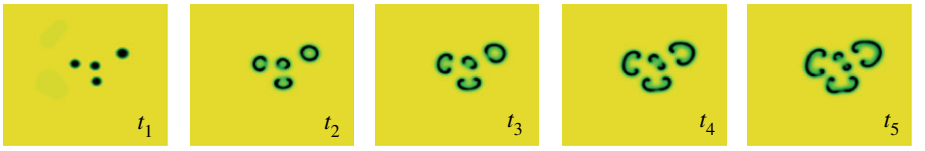


**Figure 6.** Temporal sequence of numerical simulation of the model equation (1) showing transition from localized patterns to arcs and spirals. Parameters are for $L_a = 1.25, L_1 = 2, L_2 = 2.8125, L_D = 2.5, d = 0.5$ and $\mu = 3.3$. Time runs from left to right ($t_1 < t_2 < t_3 < t_4 < t_5$). (Online version in colour.)

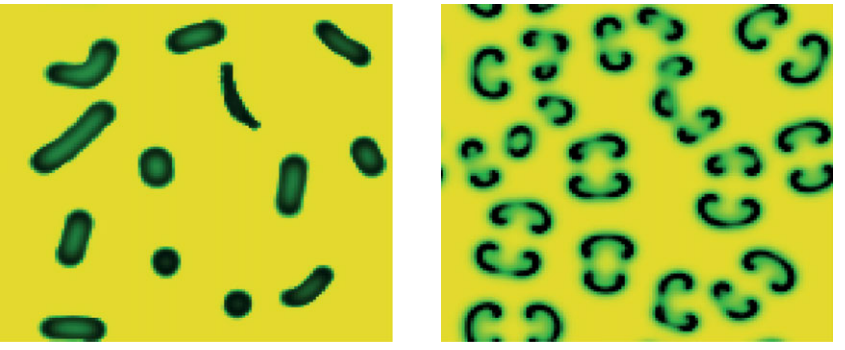

**Figure 7.** Simulation of the model equation (1) showing transitions obtained for the same parameters as in figure 6, but with different initial condition, i.e. more numerous localized patches. (Online version in colour.)

mentioning the statement made by Klausmeier in his paper: "*Numerical solution of the model shows that irregular patterns due to spatial chaos and spiral waves can arise for parameter values for which the non-spatial model has a stable limit cycle or is excitable, but these parameters are ecologically unrealistic*" [28]. This is because the Klausmeier approach is based on reaction, diffusion and advection where for some range of parameters, the model becomes excitable. In this study, equation (4.1) is not the excitable model and there is no limit cycle associated with the Andronov–Hopf bifurcation. In addition, the environmental conditions are uniform and isotropic, which is not the case for the Klausmeier model.

## 5. Conclusion

In this contribution, we have presented for the first time evidence of arcs and spiral-like vegetation patterns in strictly uniform and isotropic environmental conditions. We have used the approach based on the competitive and facilitative interactions between plants. We have first estimated the total biomass density which constitutes the only variable of the model equation (4.1). We have measured the total biomass defined as an average of the above- and below-ground biomass. We have provided measurements of the range of the facilitative interactions (radius of the aerial part of the plant) and of the competitive interaction through the roots of alfa plants (length of the plant roots). The recent campaign of field measurements has been carried out in the commune of Enjil located in the steppe plains of north-central Morocco.

Numerical simulations of the model equation (4.1) have shown evidence of arcs and spiral-like patterns that emerge as a transient behaviour and are caused by the well-known self-replication phenomenon. In the first stage, the curvature instability affects the circular shape of localized patches and leads spontaneously to the formation of arcs. In the second stage, the arcs transformed into non-rotating spirals that occupy the whole space available in a given arid landscape.

These qualitative results cast new light on the interpretation of the dynamics of tussock-forming species as alfa. The dieback in the centre of the tufts may not be a detrimental consequence of necromass accumulation as sometimes hypothesized [52] but rather a direct consequence of the dynamics of grass biomass exerting facilitative and competitive non-local interactions of distinct ranges. In our study site, the proportion of necromass is lower than mentioned in the literature, possibly because of a strong grazing pressure. This fact may explain why bare soil was frequently observed at the center of the ring-shaped or doughnut-like structures (figure 1) in agreement with simulations (figures 6 and 7). Structures of this type are barely mentioned in literature dealing with alfa (but see [49]). In the absence of model predictions, several authors may not have been deemed relevant to report and interpret similar structures. The existence of structures of different morphologies clearly supports the interpretation that tussock shapes, even circular and compact ones, may not be genetically predetermined but rather shaped by a dynamical process in interaction with the environment. This was hypothesized and modelled by [53] regarding *Festuca orthophylla* and may also apply to alfa. Since the model we use is parameterized from plant characteristic sizes (notably $L_a$), the question is: on which type of plant modules (or 'ramets') should such parameters be measured?

Parametrization obviously deserves further investigation. Moreover, two parameters were not yet measured for the alfa plants considered in this contribution: the range $L_D$ and the strength $d$ of non-local seed dispersion. More data on this ecosystem and a new campaign of field measurements and observation over long time-lapse are, however, necessary to confirm the mechanism based on the self-organization hypothesis and self-replication towards the formation of spirals and arcs. However, this simple conceptual model allows us to test a set of predictions for water-limited ecosystems. The phenomenon of arcs and spiral formations should be visible not only in Morocco but also in other arid landscapes. It is beyond the scope of this contribution to present a quantitative study. Field measurements shown in this contribution constitute the first step towards a complete parameter assessment.

Data accessibility. This article has no additional data.

Competing interests. We declare we have no competing interests.

Funding. This work is supported by Fès-Meknès Regional Council under grant number 2016/02/19. M.T. received support from the Fonds National de la Recherche Scientifique (Belgium). M.G.C. and M.T. acknowledge the support of CONICYT project REDES150046.

Acknowledgements. Stimulating discussions with René Lefever and with Jamal Ibijbijen are gratefully acknowledged. We are indebted to the 'Soil Microbiology and Environment Team' for useful help in the measurement of different parameters in the laboratory.

## References

1. Prigogine I, Lefever R. 1968 Symmetry breaking instabilities in dissipative systems. *J. Chem. Phys.* **48**, 1695–1700. (doi:10.1063/1.1668896)
2. Glansdorff P, Prigogine I. 1971 *Thermodynamic Theory of Structures, Stability and Fluctuations*. New York, NY: Wiley.
3. Nicolis G, Prigogine I. 1977 *Self-Organization in Nonequilibrium Systems*. New York, NY: Wiley.
4. Turing AM. 1952 The Chemical Basis of Morphogenesis. *Phil. Trans. R. Soc. Lond. B* **237**, 3772. (doi:10.1098/rstb.1952.0012)
5. Szalai I, Cuinas D, Takacs N, Horvath J, De Kepper P. 2012 Chemical morphogenesis: recent experimental advances in reaction-diffusion system design and control. *Interface Focus* **2**, 417–432. (doi:10.1098/rsfs.2012.0010)
6. Lefever R. 2018 The rehabilitation of irreversible processes and dissipative structures' 50th anniversary. *Phil. Trans. R. Soc. A* **376**, 20170365. (doi:10.1098/rsta.2017.0365)
7. Rosanov NN 2002. *Spatial Hysteresis and Optical Patterns*. Berlin, Germany: Springer.
8. Staliunas K, Sanchez-Morcillo VJ. 2003 *Transverse Patterns in Nonlinear Optical Resonators*. Springer Tracts in Modern Physics Vol. 188. Berlin, Germany: Springer.
9. Mandel P, Tlidi M. 2004 Transverse dynamics in cavity nonlinear optics (2000–2003). *J. Opt. B: Quant. Semiclass. Opt.* **6**, R60–R75. (doi:10.1088/1464-4266/6/9/R02)

10. Mikhailov AS, Showalter K. 2006 Control of waves, patterns and turbulence in chemical systems. *Phys. Rep.* **425**, 79–194. (doi:10.1016/j.physrep.2005.11.003)
11. Tlidi M, Kolokolnikov T, Taki M. 2007 Introduction: dissipative localized structures in extended systems. *Chaos* **17**, 037101. (doi:10.1063/1.2786709)
12. Akhmediev N, Ankiewicz A. 2008 *Dissipative Solitons: From Optics to Biology and Medicine*. Berlin, Germany: Springer.
13. Purwins HG, Bodeker HU, Amiranashvili S. 2010 Dissipative solitons. *Adv. Phys.* **59**, 485–701.
14. Ridif L, D'Odorici P, Laio F. 2011 *Noise induced phenomena in the environmental sciences*. Cambridge, UK: Cambridge University Press.
15. Descalzi O, Clerc M, Residori S, Assanto G. 2011 *Localized States in Physics: Solitons and Patterns*. New York, NY: Springer.
16. Leblond H, Mihalache D. 2013 Spatiotemporal optical solitons. *Phys. Reports* **523**, 61–126. (doi:10.1016/j.physrep.2012.10.006)
17. Tlidi M, Staliunas K, Panajotov K, Vladimiorv AG, Clerc MG. 2014 Localized structures in dissipative media: from optics to plant ecology. *Phil. Trans. R. Soc. A* **372**, 20140101. (doi:10.1098/rsta.2014.0101)
18. Tlidi M, Clerc MG. 2016 Nonlinear Dynamics: Materials, Theory and Experiments. Springer Proceedings in Physics, 173.
19. Tlidi M, Panajotov K. 2018 Cavity solitons: Dissipative structures in Nonlinear Photonics. *Rom. Rep. Phys.* **70**, 406.
20. Murray JD. 2003 *Mathematical Biology*, 3rd edn. Berlin, Germany: Springer.
21. Deneubourg JL, Goss S, Franks N, Sendova-Franks A, Detrain C, Chrétien L. 1991 The dynamics of collective sorting robot-like ants and ant-like robots. In Proc. of the first international conference on simulation of adaptive behaviour on From animals to animats, (pp. 356-363). Cambridge, MA: MIT press.
22. Goldbeter A. 1996 *Biochemical Oscillations and Cellular Rhythms*. Cambridge, UK: CUP.
23. Macfadyen WA. 1950 Vegetation patterns in the semi-desert plains of British Somaliland. *Geogr. J.* **116**, 199–211. (doi:10.2307/1789384)
24. Lefever R, Lejeune O. 1997 On the origin of tiger bush. *Bull. Math. Biol.* **59**, 263–294. (doi:10.1007/bf02462004)
25. Lejeune O, Tlidi M. 1999 A model for the explanation of vegetation stripes (tiger bush). *J. Vegetation Sci.* **10**, 201–208. (doi:10.2307/3237141)
26. Couteron P, Lejeune O. 2001 Periodic spotted patterns in semi-arid vegetation explained by a propagation-inhibition model. *J. Ecol.* **89**, 616–628. (doi:10.1046/j.0022-0477.2001.00588.x)
27. Lejeune O, Tlidi M, Lefever R. 2004 Vegetation spots and stripes: Dissipative structures in arid landscapes. *Int. J. Quantum Chem.* **98**, 261–271. (doi:10.1002/qua.10878)
28. Klausmeier CA. 1999 Regular and irregular patterns in semiarid vegetation. *Science* **284**, 1826–1828. (doi:10.1126/science.284.5421.1826)
29. HilleRisLambers R, Rietkerk M, van den Bosch F, Prins HH, de Kroon H. 2001 Vegetation pattern formation in semi-arid grazing systems. *Ecology* **82**, 50–61. (doi:10.1890/0012-9658(2001)082[0050:VPFISA]2.0.CO;2)
30. Okayasu T, Aizawa Y. 2001 Systematic analysis of periodic vegetation patterns. *Prog. Theor. Phys.* **106**, 705–719. (doi:10.1143/PTP.106.705)
31. von Hardenberg J, Meron E, Shachak M, Zarmi Y. 2001 Diversity of vegetation patterns and desertification. *Phys. Rev. Lett.* **87**, 198101. (doi:10.1103/PhysRevLett.87.198101)
32. Gilad E, von Hardenberg J, Provenzale A, Shachak M, Meron E. 2004 Ecosystems engineers: from pattern formation to habitat creation. *Phys. Rev. Lett.* **93**, 098105. (doi:10.1103/PhysRevLett.93.098105)
33. Sherratt JA. 2005 An analysis of vegetation stripe formation in semi-arid landscapes. *J. Math. Biol.* **51**, 183–197. (doi:10.1007/s00285-005-0319-5)
34. D'Odorico P, Laio F, Ridolfi L. 2006 Patterns as indicators of productivity enhancement by facilitation and competition in dryland vegetation. *J. Geophys. Res.* **111**, G03010. (doi:10.1029/2006JG000176)
35. Ridolfi L, D'Odorico P, Laio F 2011 *Noise-induced phenomena in the environmental sciences*. Cambridge, UK: Cambridge University Press.
36. Rietkerk M, Boerlijst MC, van Langevelde F, HilleRisLambers R, de Koppel JV, Kumar L, Prins HH, de Roos AM. 2002 Self-organization of vegetation in arid ecosystems. *Am. Nat.* **160**, 524–530. (doi:10.2307/3079239)

37. Lejeune O, Tlidi M, Couteron P. 2002 Localized vegetation patches: a self-organized response to resource scarcity. *Phys. Rev. E* **66**, 010901. (doi:10.1103/PhysRevE.66.010901)
38. Rietkerk M, Dekker SC, De Ruiter PC, van de Koppel J. 2004 Self-organized patchiness and catastrophic shifts in ecosystems. *Science* **305**, 1926–1929. (doi:10.1126/science.1101867)
39. Tlidi M, Lefever R, Vladimirov A. 2008 On Vegetation Clustering, Localized Bare Soil Spots and Fairy Circles. *Lect Notes Phys.* **751**, 402.
40. Bordeu I, Clerc M, Couteron P, Lefever R, Tlidi M. 2016 Self-replication of localized vegetation patches in scarce environments. *Sci. Rep.* **6**, 33703. (doi:10.1038/srep33703)
41. Tlidi M, Bordeu I, Clerc M, Escaff D. 2018 *Extended patchy ecosystems may increase their total biomass through self-replication. Ecological Indicator*. Article in Press.
42. Zhabotinsky AM, Zaikin AN. 1971 Spatial effects in a self-oscillating chemical system. In Oscillatory processes in biological and chemical systems II. (ed. EE Sel'kov) Science Publ., Puschino.
43. Winfree AT. 1972 Spiral waves of chemical activity. *Science* **175**, 634–636. (doi:10.1126/science.175.4022.634)
44. Keener JP, Tyson JJ. 1986 Spiral waves in the Belousov-Zhabotinskii reaction. *Physica D* **21**, 307–324. (doi:10.1016/0167-2789(86)90007-2)
45. Zykov VS, Mikhailov AS, Muller SC. 1998 Wave instabilities in excitable media with fast inhibitor diffusion. *Phys. Rev. Lett.* **81**, 2811. (doi:10.1103/PhysRevLett.81.2811)
46. Aidoud A, Lefloch E, Le Houérou HN. 2006 Les steppes arides du nord de l'Afrique. *Sécheresse* **17**, 19–30.
47. Aidoud A, Touffet J. 1996 La régression de l'alfa (Stipa tenacissima L.), graminée pérenne, un indicateur de désertification des steppes algériennes. *Sécheresse* **7**, 187–193.
48. Aloui K, Ksontini M, Rejeb MN. 2013 Etude des caractéristiques écologiques et de la dynamique végtative des nappes alfatiéres des monts de Maknassi en Tunisie centrale. *Annales de l'inrgref* **18**, 213–223.
49. Cerda A. 1997 The effect of patchy distribution of Stipa tenacissima L. on runoff and erosion. *J. Arid Environ.* **36**, 37–51. (doi:10.1006/jare.1995.0198)
50. Gauquelin T, Jalut G, Iglesias M, Valle F, Fromard F, Dedoubat JJ. 1996 Phytomass and carbon storage in the Stipa tenacissima steppes of the Baza basin Andalusia, Spain. *J. Arid Environ.* **34**, 277–286. (doi:10.1006/jare.1996.0109)
51. Rhanem M. 2009 L'alfa (Stipa tenacissima L.) dans la plaine de Midelt (Haut Bassin versant de la Moulaya, Maroc), éléments de climatologie. *Physio-Géo-Géographie Physique et Environnement*, **III**, 1–20. (doi:10.4000/physio-geo.696)
52. Hellal B, Ayad N, Maatoug M, Boularas M. 2007 Influence du fatras sur la biomasse foliaire de l'alfa (Stipa tenacissima *L.*) de la steppe du Sud oranais (Algérie occidentale). *Sécheresse* **1**, 65–71.
53. Couteron P, Anthelme F, Clerc M, Escaff D, Fernandez-Oto C, Tlidi M. 2014 Plant clonal morphologies and spatial patterns as self-organized responses to resource-limited environments. *Phil. Trans. R. Soc. A*, **372**, 20140102. (doi:10.1098/rsta.2014.0102)
54. Barbier N, Couteron P, Lejoly J, Deblauwe V, Lejeune O. 2006 Self-organized vegetation patterning as a fingerprint of climate and human impact on semi-arid ecosystems. *J. Ecol.* **94**, 537–547. (doi:10.1111/j.1365-2745.2006.01126.x)
55. Barbier N, Couteron P, Lefever R, Deblauwe V, Lejeune O. 2008 Spatial decoupling of facilitation and competition at the origin of gapped vegetation patterns. *Ecology* **89**, 1521–1531. (doi:10.1890/07-0365.1)
56. Lefever R, Barbier N, Couteron P, Lejeune O. 2009 Deeply gapped vegetation patterns: on crown/root allometry, criticality and desertification. *J. Theor. Biol.* **261**, 194–209. (doi:10.1016/j.jtbi.2009.07.030)
57. Lefever R, Turner JW. 2012 A quantitative theory of vegetation patterns based on plant structure and the non-local F-KPP equation. *Comptes Rendus Mécanique* **340**, 818–828. (doi:10.1016/j.crme.2012.10.030)
58. Hogeweg P. 1988 Cellular automata as a paradigm for ecological modeling. *Appl. Math. Comput.* **27**, 81–100. (doi:10.1016/0096-3003(88)90100-2)
59. Green DG. 1994 Connectivity and complexity in landscapes and ecosystems. *Pacific Conserv. Biol.* **1**, 194–200. (doi:10.1071/PC940194)
60. Thiery JM, d'Herbes JM, Valentin C. 1995 A model simulating the genesis of banded vegetation patterns in Niger. *J. Ecol.* **83**, 497–507. (doi:10.2307/2261602)

61. Dunkerley DL. 1997 Banded vegetation: development under uniform rainfall from a simple cellular automaton model. *Plant Ecol.* **129**, 103–111. (doi:10.1023/A:1009725732740)
62. Boaler SB, Hodge CAH. 1964 Observations on vegetation arcs in the northern region, Somali Republic. *J. Ecol.* **52**, 511–544. (doi:10.2307/2257847)
63. Worrall GA. 1959 The Butana grass patterns. *Eur. J. Soil Sci.* **10**, 34–53. (doi:10.1111/j.1365-2389.1959.tb00664.x)
64. Wickens GE, Collier FW. 1971 Some vegetation patterns in the Republic of the Sudan. *Geoderma*, **6**, 43–59. (doi:10.1016/0016-7061(71)90050-4 )